



Broad Anti-coronavirus Activity of Food and Drug Administration-Approved Drugs against SARS-CoV-2 *In Vitro* and SARS-CoV *In Vivo*

Stuart Weston,^a Christopher M. Coleman,^{a*} Robert Haupt,^a  James Logue,^a Krystal Matthews,^a Yize Li,^b Hanako M. Reyes,^b Susan R. Weiss,^b  Matthew B. Frieman^a

^aDepartment of Microbiology and Immunology, University of Maryland School of Medicine, Baltimore, Maryland, USA

^bDepartment of Microbiology, Perelman School of Medicine at the University of Pennsylvania, Philadelphia, Pennsylvania, USA

ABSTRACT Severe acute respiratory syndrome coronavirus 2 (SARS-CoV-2) emerged in China at the end of 2019 and has rapidly caused a pandemic, with over 20 million recorded COVID-19 cases in August 2020 (<https://covid19.who.int/>). There are no FDA-approved antivirals or vaccines for any coronavirus, including SARS-CoV-2. Current treatments for COVID-19 are limited to supportive therapies and off-label use of FDA-approved drugs. Rapid development and human testing of potential antivirals is urgently needed. Numerous drugs are already approved for human use, and subsequently, there is a good understanding of their safety profiles and potential side effects, making them easier to fast-track to clinical studies in COVID-19 patients. Here, we present data on the antiviral activity of 20 FDA-approved drugs against SARS-CoV-2 that also inhibit SARS-CoV and Middle East respiratory syndrome coronavirus (MERS-CoV). We found that 17 of these inhibit SARS-CoV-2 at non-cytotoxic concentrations. We directly followed up seven of these to demonstrate that all are capable of inhibiting infectious SARS-CoV-2 production. Moreover, we evaluated two of these, chloroquine and chlorpromazine, *in vivo* using a mouse-adapted SARS-CoV model and found that both drugs protect mice from clinical disease.

IMPORTANCE There are no FDA-approved antivirals for any coronavirus, including SARS-CoV-2. Numerous drugs are already approved for human use that may have antiviral activity and therefore could potentially be rapidly repurposed as antivirals. Here, we present data assessing the antiviral activity of 20 FDA-approved drugs against SARS-CoV-2 that also inhibit SARS-CoV and MERS-CoV *in vitro*. We found that 17 of these inhibit SARS-CoV-2, suggesting that they may have pan-anti-coronavirus activity. We directly followed up seven of these and found that they all inhibit infectious-SARS-CoV-2 production. Moreover, we evaluated chloroquine and chlorpromazine *in vivo* using mouse-adapted SARS-CoV. We found that neither drug inhibited viral replication in the lungs, but both protected against clinical disease.

KEYWORDS FDA-approved drugs, SARS-CoV-2, antiviral therapeutics, coronavirus, drug repurposing, nCoV-2019, pandemic

At the end of December 2019, reports started to emerge from China of patients suffering from pneumonia of unknown etiology. By early January, a new coronavirus had been identified and determined to be the cause (1). Since then, the virus, originally known as novel coronavirus 2019 (nCoV-2019) and now designated severe acute respiratory syndrome coronavirus 2 (SARS-CoV-2), has spread around the world. In August 2020, over 20 million confirmed cases of COVID-19 (the disease caused by SARS-CoV-2 infection) had been reported, resulting in over 700,000 deaths (<https://covid19.who.int/>). Multiple countries have enacted social distancing and quarantine

Citation Weston S, Coleman CM, Haupt R, Logue J, Matthews K, Li Y, Reyes HM, Weiss SR, Frieman MB. 2020. Broad anti-coronavirus activity of Food and drug Administration-approved drugs against SARS-CoV-2 *in vitro* and SARS-CoV *in vivo*. *J Virol* 94:e01218-20. <https://doi.org/10.1128/JVI.01218-20>.

Editor Julie K. Pfeiffer, University of Texas Southwestern Medical Center

Copyright © 2020 American Society for Microbiology. All Rights Reserved.

Address correspondence to Matthew B. Frieman, MFrieman@som.umaryland.edu.

* Present address: Christopher M. Coleman, School of Life Sciences, University of Nottingham, Queen's Medical Centre, Nottingham, United Kingdom.

Received 16 June 2020

Accepted 14 August 2020

Accepted manuscript posted online 19 August 2020

Published 14 October 2020

measures, attempting to reduce person-to-person transmission of the virus. Health care providers lack pharmaceutical countermeasures against SARS-CoV-2, beyond public health interventions, and there remains a desperate need for rapid development of antiviral therapeutics. A potential route to candidate antivirals is through repurposing of already approved drugs (for reviews, see references 2–4, and for examples, see references 5–8). We previously screened a library of FDA-approved drugs for antiviral activity against two other highly pathogenic human coronaviruses, SARS-CoV and Middle East respiratory syndrome coronavirus (MERS-CoV) (6). We found 27 drugs that inhibited replication of both of these coronaviruses, suggesting that they may have broad anti-coronaviral activity. One of the hits from that work was imatinib, and we subsequently determined its mechanism of action by demonstrating that this drug inhibits fusion of coronaviruses with cellular membranes, thus blocking entry (9, 10).

Here, we present our investigation of 20 priority compounds from our previous screening to test if they can also inhibit SARS-CoV-2. Since these compounds are already approved for use in humans, they make ideal candidates for drug repurposing and rapid development as antiviral therapeutics. Our work found that 17 of the 20 tested drugs that inhibited SARS-CoV and MERS-CoV could also inhibit SARS-CoV-2, with similar half-maximal inhibitory concentrations (IC_{50} s). We further assessed a subset of these drugs for their effects on SARS-CoV-2 RNA and infectious virus production and found all to have inhibitory activity *in vitro*. Our screening based on cytopathic effect therefore appears to be a favorable approach to find drugs capable of inhibiting production of infectious virus. Currently there are no well-established small animal model systems for SARS-CoV-2. However, there is a well-established mouse-adapted system for SARS-CoV (MA15 strain) (11), and we present data here assessing the *in vivo* efficacy of chloroquine (CQ) and chlorpromazine (CPZ) against SARS-CoV. We found that drug treatment does not inhibit virus replication in mouse lungs but does improve clinical outcome.

RESULTS

Screening FDA-approved compounds for anti-SARS-CoV-2 activity. Previously, we performed a large-scale drug screen on 290 FDA-approved compounds to investigate which may have antiviral activity against SARS-CoV and MERS-CoV (6). With the emergence of SARS-CoV-2, we prioritized testing 20 of the 27 hits that were determined to inhibit both of the previously tested coronaviruses for antiviral activity against the novel virus. The list of tested compounds is shown in Table 1. Our screening started at 50 μ M and used an 8-point, 1:2 dilution series with infections being performed at a multiplicity of infection (MOI) of either 0.01 or 0.004. CellTiter-Glo (CTG) assays were performed 3 days post-infection (dpi) to determine relative cell viability between drug and vehicle control treated cells. Uninfected samples were used to measure the cytotoxicity of drug alone. From the relative luminescence data of the CTG assay, percent inhibition (of cell death caused by viral infection) could be measured and plotted along with the percent cytotoxicity of drug alone. Figure 1 shows the plotted graphs from one representative of three independent screens at an MOI of 0.01. For drugs demonstrating a cell toxicity rate lower than 30%, we were able to calculate IC_{50} s at both MOI from these graphs for 17 of the 20 drugs (summarized in Table 1).

Drug screen validation. In order to validate our screening process as a means to identify compounds with antiviral effect, we decided to follow up with a subset of drugs. Chloroquine (CQ) has become the source of much interest as a potential treatment for COVID-19 (12); as such, we further investigated hydroxychloroquine (HCQ) and CQ, as both were present in our screen (Table 1). Vero E6 cells were plated and pretreated with drug for 2 h prior to infection with SARS-CoV-2 at an MOI of 0.1. Supernatant was collected 24 h post-infection (hpi) to determine titer of virus by TCID₅₀ (50% tissue culture infective dose) assay, and cells were collected in TRIzol to assess production of viral mRNA. Treatment with both drugs caused a significant reduction in viral mRNA levels, especially at higher concentrations, without drug-induced cytotoxicity (Fig. 1 and Table 1). There was a significant decrease in relative expression levels

TABLE 1 IC₅₀s and CC₅₀s for 20 FDA-approved drugs against SARS-CoV-2^a

Drug	MOI	No. of plate replicates ^b	IC ₅₀ (avg)	CC ₅₀ (avg)	SI (avg)
Amodiaquine dihydrochloride dihydrate	0.004	2, 3	2.59	34.42	13.31
	0.01	3	4.94	34.42	6.97
Amodiaquine hydrochloride	0.004	3	2.36	>38.63 ^c	>16.37 ^c
	0.01	3	5.64	>38.63 ^c	>6.84 ^c
Anisomycin	0.004	3	ND	<0.39	ND
	0.01	3	ND	<0.39	ND
Benztropine mesylate	0.004	3	13.8	>>50 ^d	>>3.62 ^d
	0.01	2, 3	17.79	>>50 ^d	>>2.81 ^d
Chloroquine phosphate	0.004	3	42.03	>50 ^c	>1.19 ^c
	0.01	3	46.8	>50 ^c	>1.07 ^c
Chlorpromazine hydrochloride	0.004	2, 3	3.14	11.88	3.78
	0.01	2, 3	4.03	11.88	2.94
Clomipramine hydrochloride	0.004	2, 3	5.63	>29.68 ^c	>5.27 ^c
	0.01	3	7.59	>29.68 ^c	>3.91 ^c
Emetine dihydrochloride hydrate	0.004	3	ND	<0.39	ND
	0.01	2, 3	ND	<0.39	ND
Fluphenazine dihydrochloride	0.004	3, 2	6.36	20.02	3.15
	0.01	2	8.98	20.02	2.23
Fluspirilene	0.004	3	3.16	30.33	9.61
	0.01	3	5.32	30.33	5.71
Gemcitabine hydrochloride	0.004	3	ND	23.22	ND
	0.01	3	ND	23.22	ND
Hydroxychloroquine sulfate	0.004	3	9.21	>>50 ^d	>>5.43 ^d
	0.01	3	11.17	>>50 ^d	>>4.48 ^d
Imatinib mesylate	0.004	3	3.24	>30.86 ^c	>9.52 ^c
	0.01	3	5.32	>30.86 ^c	>5.80 ^c
Mefloquine hydrochloride	0.004	3	7.11	18.53	2.61
	0.01	3	8.06	18.53	2.3
Promethazine hydrochloride	0.004	3	9.21	>42.59 ^c	>4.62 ^c
	0.01	3	10.44	>42.59 ^c	>4.08 ^c
Tamoxifen citrate	0.004	2	34.12	37.96	1.11
	0.01	1, 2	8.98	37.96	4.23
Terconazole	0.004	3	11.92	41.46	3.48
	0.01	2, 3	16.14	41.46	2.57
Thiethylperazine maleate	0.004	3	7.09	18.37	2.59
	0.01	3	8.02	18.37	2.29
Toremifene citrate	0.004	2, 3	4.77	20.51	4.3
	0.01	3	11.3	20.51	1.81
Triparanol	0.004	2, 3	4.68	21.21	4.53
	0.01	2, 3	6.41	21.21	3.31

^aAbbreviations: MOI, multiplicity of infection; IC₅₀, half-maximal inhibitory concentration; CC₅₀, half-maximal cytotoxic concentration; ND, not determined.

^bWhere there are two run totals, they are listed in the order IC₅₀, CC₅₀.

^cAt least one CC₅₀ could be extrapolated from the curve fit, suggesting that toxicity and SI are slightly higher than listed.

^dNo CC₅₀ could be extrapolated from the curve fit, suggesting that toxicity and SI are much higher than listed.

of both RNA-dependent RNA polymerase (RdRp) and nucleoprotein (N) mRNA across the range of concentrations used (Fig. 2A to D). Along with causing a reduction in viral mRNA, treatment with both drugs caused a significant reduction in viral replication (Fig. 2E and F). SARS-CoV-2 production was more sensitive to HCQ than CQ, with larger inhibition seen at the same concentration of treatment, which is in agreement with HCQ having a lower IC₅₀ in our cell viability assay (Table 1). We also performed a time-of-addition assay with the highest concentration of HCQ to investigate whether SARS-CoV-2 entry was the point of inhibition of this compound (Fig. 2G). Interestingly, while the addition of HCQ at 2 hpi did result in some reduction in inhibitory activity, there was not a complete loss, suggesting that HCQ treatment may impact other stages of the viral life cycle than just entry.

We previously used a β -lactamase-Vpr chimeric protein (Vpr-BlaM) pseudotype system to demonstrate that imatinib (a drug also seen to inhibit SARS-CoV-2 [Table 1 and Fig. 1]) inhibits SARS-CoV and MERS-CoV spike-mediated entry (9). We used this

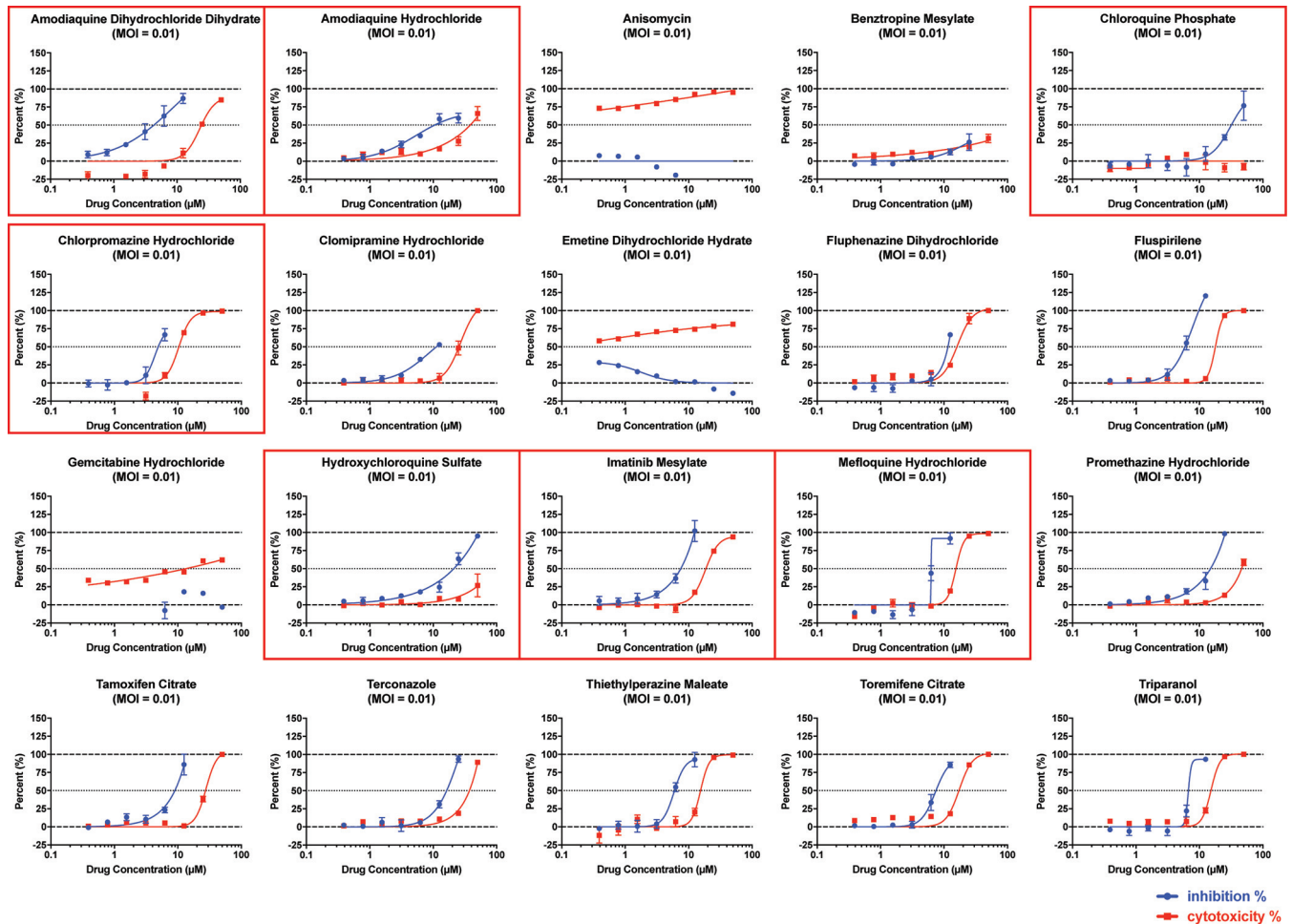


FIG 1 Percentage inhibition and percentage cytotoxicity graphs from drug screens starting at 50 μM using an 8-point, 1:2 dilution series. Results are from one representative drug screen of three showing percentage inhibition and cytotoxicity for each of the tested drugs. Triplicate wells of cells were pretreated with the indicated drug for 2 h prior to infection with SARS-CoV-2 at an MOI of 0.01. Cells were incubated for 72 h prior to CellTiter-Glo assays to assess cytopathic effect. Data are percent inhibition of relative cell viability for drug-treated cells versus vehicle control. The values are means, with error bars displaying standard deviation between the triplicate wells. Seven graphs are boxed in red to highlight drugs that become the subject of follow-up study.

system to more directly investigate whether CQ could inhibit viral entry mediated by coronavirus spike, and we additionally included chlorpromazine (CPZ), as it is known to inhibit clathrin-mediated endocytosis (13) and was also part of our drug screening (Table 1 and Fig. 1). In this assay, when the pseudovirus fuses with a cellular membrane, BlaM is released into the cytoplasm of the infected cell. BlaM cleaves cytoplasmic loaded CCF2 to change its emission spectrum from 520 nm (green) to \sim 450 nm (blue), which can be quantified by flow cytometry.

Cells were treated with CQ or CPZ for 1 h before infection with BlaM-containing SARS-CoV spike (SARS-S) pseudovirions (PV). Cells were then analyzed by flow cytometry to quantify the cleavage of CCF2. In mock-treated cells infected with SARS-S PV, there was a shift in the CCF2 emission spectrum, indicating that BlaM had been released to the cytosol and that spike-mediated fusion with cellular membranes had occurred. Upon treatment with CQ or CPZ, there was a $>90\%$ reduction in CCF2 cleavage caused by SARS-S PV (Fig. 2H). These data demonstrate that both drugs inhibit SARS-CoV spike-mediated fusion with cellular membranes. These pseudovirus assays suggest that the inhibition of coronavirus replication caused by CQ and CPZ is at the stage of entry into cells, but when these results are combined with those of the time-of-addition assays (Fig. 2G), there is a suggestion that later stages may also be impacted.

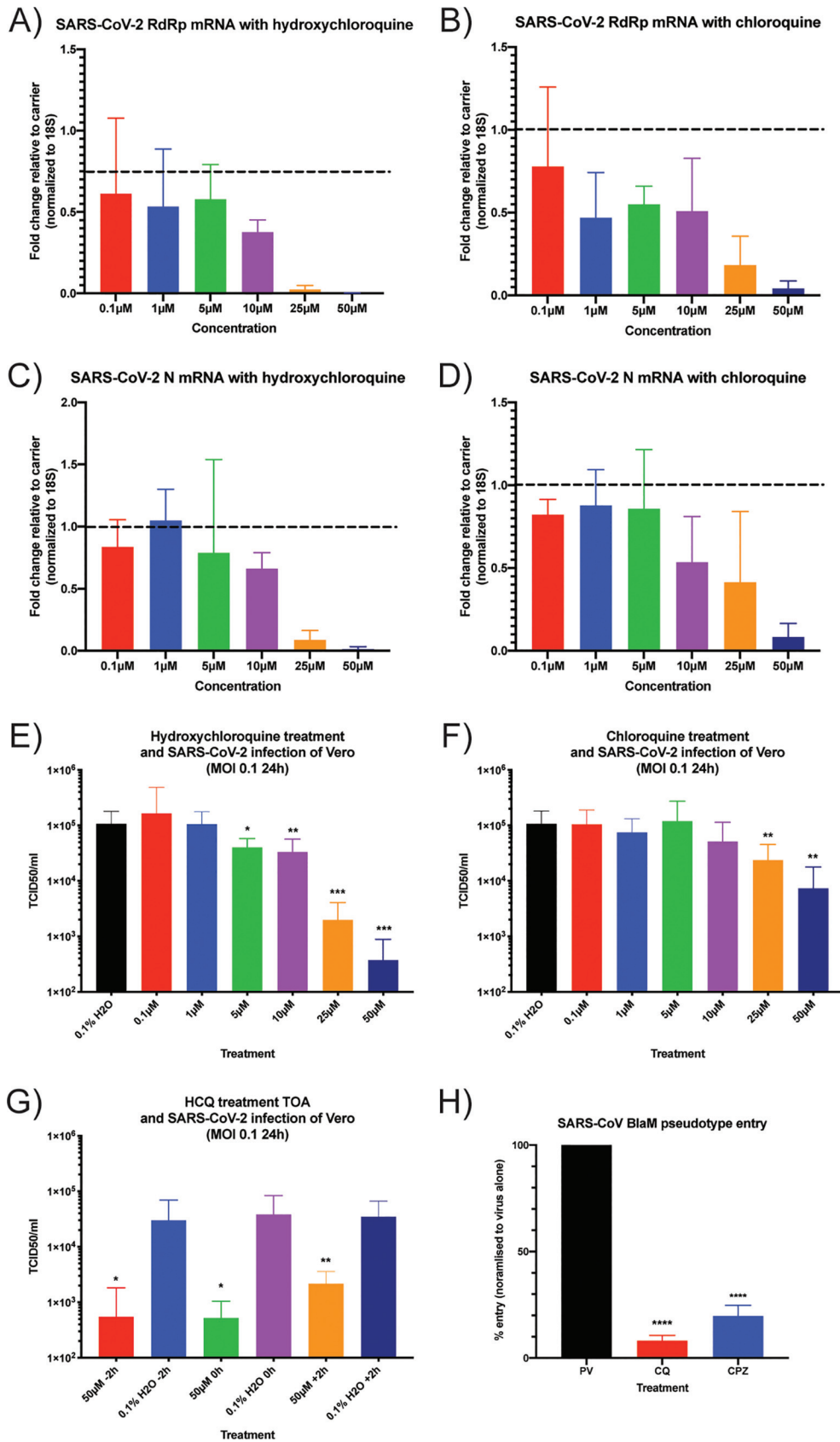


FIG 2 Hydroxychloroquine and chloroquine inhibit production of SARS-CoV-2 N and RdRp mRNA. Vero E6 cells were pretreated with hydroxychloroquine sulfate (A, C, and E) or chloroquine phosphate (B, D, and F) at the indicated (Continued on next page)

HCQ and CQ are used as antimalarial drugs and are in the class of aminoquinolines, which are hemozoin inhibitors. Interestingly, from our drug screening, three other hemozoin inhibitors were identified: amodiaquine dihydrochloride dihydrate, amodiaquine hydrochloride, and mefloquine. We therefore decided to directly test these drugs for antiviral activity against SARS-CoV-2. We directly tested CPZ against SARS-CoV-2, having seen that it could inhibit SARS-CoV S-mediated entry into cells (Fig. 2H). We also included imatinib, since we had previously shown that it can inhibit entry of both SARS-CoV and MERS-CoV (9) and was a hit against SARS-CoV-2 (Fig. 1 and Table 1). Again, Vero E6 cells were pretreated with drugs at various concentrations and infected with SARS-CoV-2 at an MOI of 0.1 for 24 h, after which supernatant samples were collected. As can be seen in Fig. 3, at the highest concentrations of all drugs there was significant inhibition of SARS-CoV-2 infection. All five drugs showed high levels of inhibition at a non-cytotoxic concentration of 20 μ M (see Fig. 1 for toxicity data).

Overall, the data from Fig. 2 and 3 indicate that there are various FDA-approved drugs that have broad-spectrum anti-coronavirus activity *in vitro* and that our initial screening based on cytopathic effect is a good method to identify compounds with antiviral activity.

FDA-approved drugs inhibit SARS-CoV-2 replication in human A549 cells. Our screening and subsequent initial follow-up were performed in Vero E6 cells, which are an African green monkey kidney epithelial cell line. We also wanted to determine whether the selected 7 drugs in our follow-up inhibited SARS-CoV-2 replication in a human cell line. For this, we used A549 lung adenocarcinoma cells that stably express human ACE2 (A549-hACE2), the SARS-CoV-2 receptor protein. As before, cells were pretreated with each compound for 2 h using a single dose point (50 μ M for HCQ and CQ and 20 μ M for the other 5) and then infected with SARS-CoV-2. We found in these cells that peak titer was achieved at 48 hpi; therefore, supernatant was collected at this time point and used to determine titers of released virus, and cells were collected in TRIzol for RNA expression analysis. All 7 of these drugs were capable of causing a significant reduction in replication of SARS-CoV-2 in A549 cells, in terms of both RNA production for both RdRp and N genes (Fig. 4A and B) and infectious virus production (Fig. 4C). These data show that these 7 FDA-approved drugs are able to inhibit *in vitro* replication of SARS-CoV-2 in human cells.

Chloroquine and chlorpromazine do not inhibit SARS-CoV (MA15) replication in mouse lungs but significantly reduce weight loss and clinical signs. CQ and CPZ treatment displayed significant inhibition of coronavirus replication *in vitro*, with our data suggesting that entry is inhibited. We therefore decided to investigate whether these drugs were efficacious *in vivo* using the SARS-CoV strain MA15 in BALB/c mice (11). There is currently no well-established SARS-CoV-2 small animal model, and therefore, we used SARS-CoV MA15 as a surrogate. Since we think that CQ and CPZ impact

FIG 2 Legend (Continued)

concentration (or 0.1% water as a vehicle control) for 2 h prior to infection with SARS-CoV-2 at an MOI of 0.1. Cells were collected in TRIzol 24 hpi. RNA was extracted from the TRIzol sample, and qRT-PCR was performed for viral RdRp (A and B) or N (C and D) mRNA using WHO primers. RNA levels were normalized with 18S RNA, and fold change for drug-treated cells relative to vehicle control was calculated (dotted lines indicate a fold change of 1, which is no change over control). Data are from 3 independent infections performed on triplicate wells; the fold change was calculated in each independent experiment, and the mean fold change is plotted, with error bars displaying standard deviations. Along with TRIzol samples for RNA, supernatant was collected from cells and used for TCID₅₀ assays to determine infectious-virus production following treatment with HCQ (E) or CQ (F). Data are from 3 independent infections performed on triplicate wells, with the TCID₅₀ per milliliter being averaged across all wells. Error bars show standard deviations. (G) Cells were treated with 50 μ M HCQ or 0.1% water as a control. Drug was added either at 2 h prior to infection, at the time of infection, or at 2 h after infection with SARS-CoV-2 at an MOI of 0.1. After 24 h infection, supernatant was collected and used for TCID₅₀ assays to determine infectious-virus production. Data are from 3 independent infections performed on triplicate wells, with the values being averaged across all wells. Error bars show standard deviations. (H) SARS-CoV spike pseudoviruses (PV) were used for infection of BSC1 cells. The cells were treated with 10 μ M CQ or CPZ for 1 h prior to infection with PV for 3 h. The PV carry BlaM, and cells were loaded with CCF2 to monitor cleavage and shift in fluorescence output for evidence of S-mediated entry into cells. Data are normalized to those for PV alone and are from 3 independent experiments, with error bars representing standard deviations. In all cases, *t* tests were performed for vehicle control versus drug-treated samples, *, *P* < 0.05; **, *P* < 0.01; ***, *P* < 0.001; ****, *P* < 0.0001.

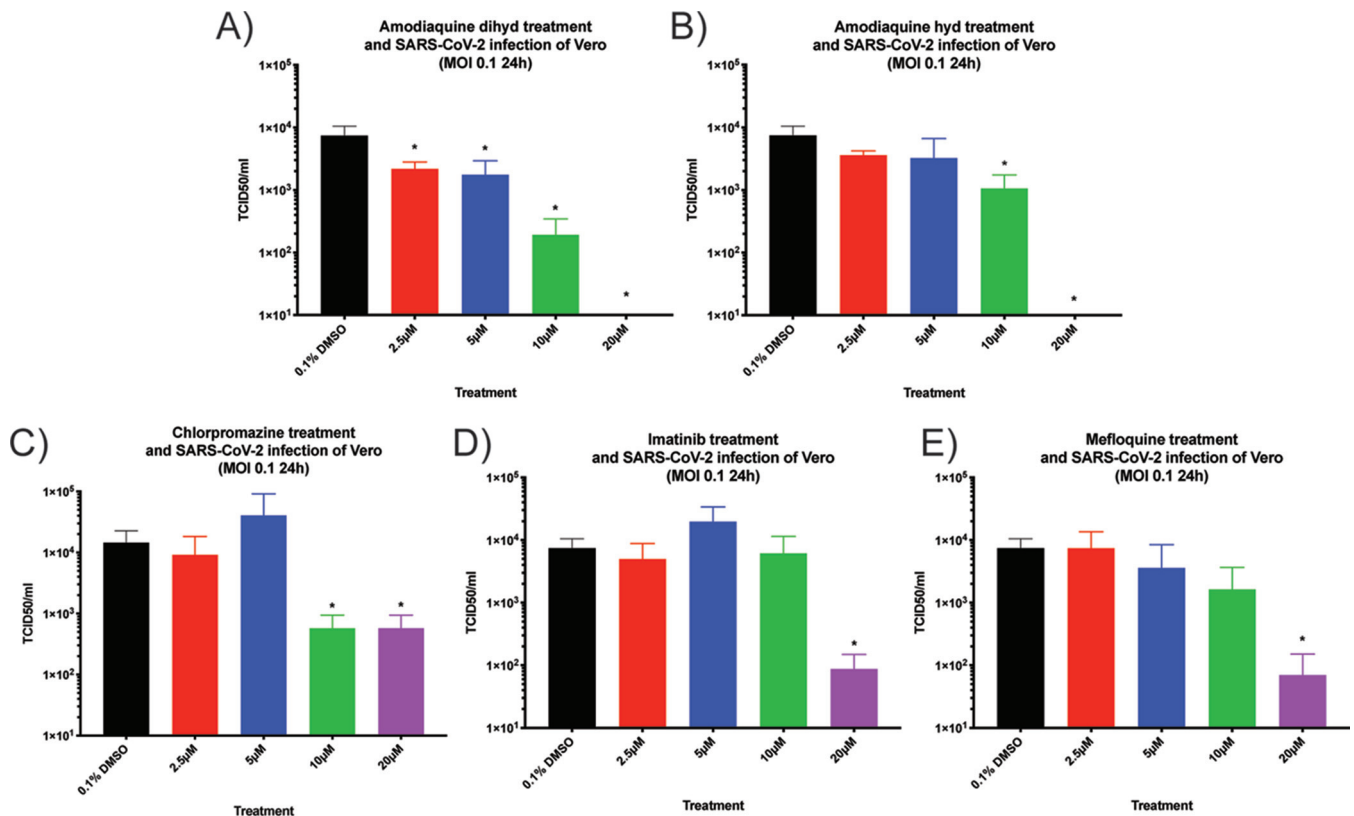


FIG 3 Antiviral activity of additional FDA-approved compounds against SARS-CoV-2. Other drugs that showed antiviral activity in our initial CellTiter-Glo screening were tested for inhibition of productive virus infection. Cells were treated with the indicated concentrations of amodiaquine dihydrochloride dihydrate (A), amodiaquine hydrochloride (B), chlorpromazine (C), imatinib (D), and mefloquine (E) for 2 h prior to infection with SARS-CoV-2 at an MOI of 0.1 for 24 h. Supernatant was collected and used for TCID₅₀ assays to quantify infectious virus production. Data are from a representative experiment of four performed on triplicate wells. Data are means, with error bars indicating standard deviations. In all cases, *t* tests were performed for vehicle control versus drug-treated samples, *, *P* < 0.05.

entry and that both viruses use the same cellular receptor of ACE2 (14–17), we believe this to be a good model. The MA15 model displays ~15 to 20% weight loss by 4 dpi, occasionally resulting in death. We tested whether prophylactically administered CQ or CPZ could protect mice from severe MA15 infection. Mice were injected intraperitoneally with either water, 0.8 mg CQ, 1.6 mg CQ, 20 µg CPZ, 100 µg CPZ, or 200 µg CPZ at day –1 of infection and then were dosed every day through the 4 days of infection. On day 0, mice were intranasally infected with 2.5×10^3 PFU of MA15 virus or phosphate-buffered saline (PBS) as a control. Weight loss was measured as a correlate of disease, and mice were euthanized at 4 dpi for analysis.

PBS-inoculated mice showed no weight loss or clinical signs of disease when treated with either water, CQ, or CPZ over the experiment time course, indicating that drug treatment did not adversely affect morbidity (Fig. 5A). Mice that were infected with MA15 and treated with water lost ~15% of their starting body weight over 4 days and had significant clinical signs of disease, including ruffled fur, labored breathing, and lethargy (Fig. 5A and 6A). Mice that were treated with 0.8 mg of CQ each day displayed weight loss similar to that seen with the water control through the first 3 days of infection; however, by 4 dpi, the weight loss was halted in the drug-treated mice (Fig. 5A). Mice that were treated with 1.6 mg CQ per day showed markedly reduced weight loss compared to the water control (Fig. 5A). Pathological analysis was also performed on hematoxylin-and-eosin (H&E)-stained sections. Mice infected with MA15 and treated with water displayed significant inflammation and denuding bronchiolitis, suggesting severe disease (Fig. 5B). In contrast, the 0.8-mg-CQ group had moderate inflammation that was reduced compared to that in controls, and the 1.6-mg group had minimal lung

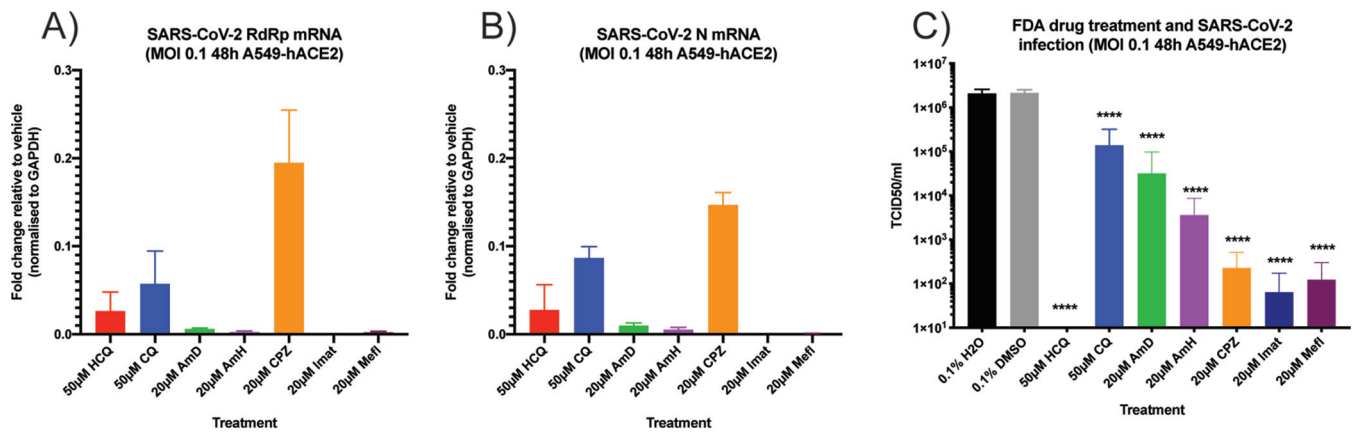


FIG 4 Antiviral activity of selected FDA-approved drugs in A549-hACE2 cells infected with SARS-CoV-2. A549-hACE2 cells were pretreated with hydroxychloroquine (HCQ), chloroquine (CQ), amodiaquine dihydrochloride dihydrate (AmD), amodiaquine hydrochloride (AmH), chlorpromazine (CPZ), imatinib (Imat), or mefloquine (Mefl) at the indicated concentrations for 2 h prior to infection with SARS-CoV-2 at MOI 0.1. At 48 hpi, supernatant was collected for titer determination by TCID₅₀ assay, and cells were collected in TRIzol for RNA extraction and qRT-PCR. qRT-PCR was carried out for the RdRp gene (A) and the N gene (B), and data are presented as fold change relative to vehicle control (0.1% H₂O for HCQ and CQ and 0.1% DMSO for all other drugs), with RNA levels being normalized to GAPDH. Data are from a representative experiment of three performed in triplicate. Error bars indicate standard deviations. (C) Titers of virus produced from drug-treated and vehicle control cells, presented as TCID₅₀/ml. Data are from three independent experiments performed in triplicate. Error bars indicate standard deviations. *t* tests were performed for vehicle control versus drug-treated samples, ****, *P* < 0.001.

pathology (Fig. 5B). Interestingly, even though CQ treatment appeared to protect against weight loss and inflammation in the lungs, the viral titer was equivalent between drug-treated and vehicle control mice (Fig. 5C).

Similar to the CQ results, CPZ treatment reduced weight loss in mice infected with MA15 at 100 µg and 200 µg, but the 20-µg treatment group was equivalent to the vehicle control group (Fig. 6A), and the H&E sections showed protection against inflammation and denuding bronchiolitis at the higher doses (Fig. 6B). Again, as with CQ treatment, even though there were reduced signs of infection with CPZ treatment, there was no difference in MA15 titer in the mouse lungs (Fig. 6C). Overall, these data indicate that even though CQ and CPZ treatment do not inhibit viral replication in the lungs, both can protect mice from signs of disease following SARS-CoV (MA15) infection.

DISCUSSION

The SARS-CoV-2 pandemic has demonstrated the desperate need for antiviral drugs. Since the emergence of SARS-CoV in 2002, research has uncovered many details of coronavirus biology and pathogenesis; however, there are currently no approved therapeutics against this emerging virus family. Whether they are used for treating SARS-CoV-2 in this current pandemic or for the next unknown viral pathogen, we must attempt to develop and validate antiviral drugs that are ready to be used at the first signs of an outbreak. Many FDA-approved drugs have been found to have antiviral activity in addition to their approved use (for examples, see references 5–8), and since these are extensively used in humans for other conditions, they could be streamlined for rapid approval and repurposing as antivirals. In our previous work, 290 FDA approved drugs were screened for antiviral activity, and 27 were found to inhibit both SARS-CoV and MERS-CoV (6). We prioritized testing these for antiviral activity against SARS-CoV-2, since they displayed broad anti-coronaviral activity. From multiple independent screens performed with two MOI, we found that 17 of our 20 tested priority compounds display significant antiviral activity at noncytotoxic concentrations. Many of the compounds have IC₅₀s under 10 µM, and these will be the source of follow-up testing on additional cell lines and in small animal models of SARS-CoV-2 and in combinatorial studies.

We further investigated seven of the hits to directly test if they inhibited SARS-CoV-2 replication. We performed follow-up experiments with HCQ, CQ, amodiaquine, and

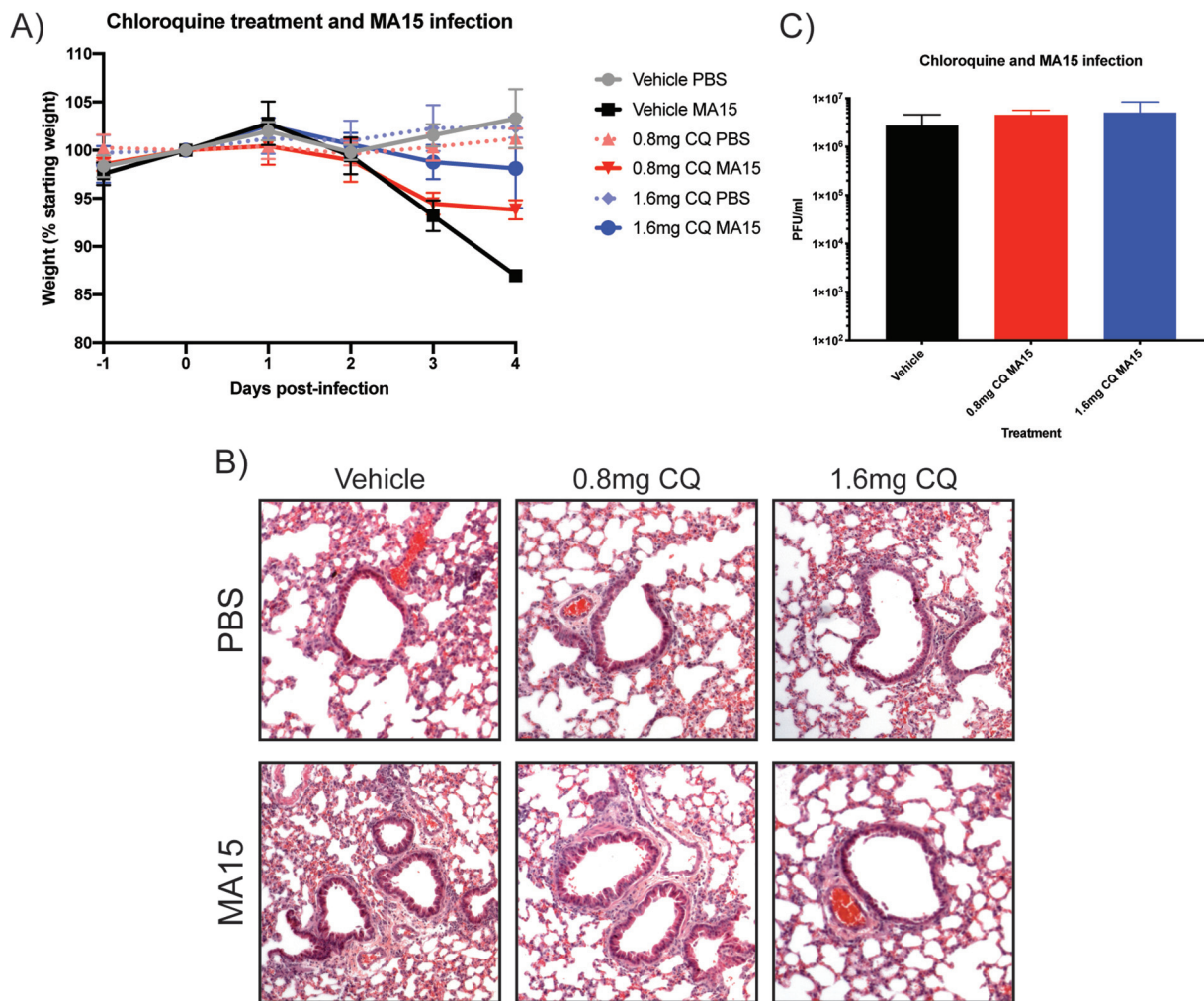


FIG 5 CQ is protective against SARS-CoV (MA15) disease *in vivo* but does not inhibit viral replication. Mice were treated with CQ 1 day prior to infection with SARS-CoV (MA15) and dosed across the 4-day infection time course. Water was used as the vehicle control, and PBS was used as a control for uninfected mice. (A) Weight loss of mice treated with CQ at two different doses (0.8 mg and 1.6 mg) over the 4-day infection. Data are presented as relative weight loss compared to the mouse weight on day 0. In each treatment group there were 5 mice, and the data are means and standard deviations. (B) At day 4, mice were euthanized, and lung sections were used for H&E staining. (C) In addition to collecting lungs for section staining, there was also collection to determine titer of virus by plaque assay.

mefloquine, because chloroquine has garnered much interest as a potential treatment for COVID-19 (12) and the others are similarly used as antimalarial drugs (18). In addition, we previously demonstrated that imatinib is an inhibitor of SARS-CoV, MERS-CoV, and infectious bronchitis virus entry into cells (9, 10), so we included it here, as its mechanism of coronavirus inhibition is understood. Finally, CPZ inhibits clathrin function in cells (13), so it can disrupt infection by many viruses that require clathrin-mediated endocytosis, and it was therefore also chosen for further analysis. Treatment of cells with all of these drugs showed inhibition of infectious viral particle production (measured by TCID₅₀ assay) at non-cytotoxic levels.

Having demonstrated that HCQ, CQ, and CPZ can inhibit cytopathic effect, mRNA synthesis, and infectious viral particle production of SARS-CoV-2, we used a previously published system of SARS-CoV pseudotype viruses carrying Vpr-BlaM to investigate whether CQ and CPZ inhibit coronavirus spike-mediated entry to better define mechanism of action. We previously used this system to define imatinib as an entry inhibitor of these viruses (9) and found similar results for CQ and CPZ, thus better defining their mechanism of antiviral activity.

Finally, we investigated the efficacy of CQ and CPZ with an *in vivo* model using

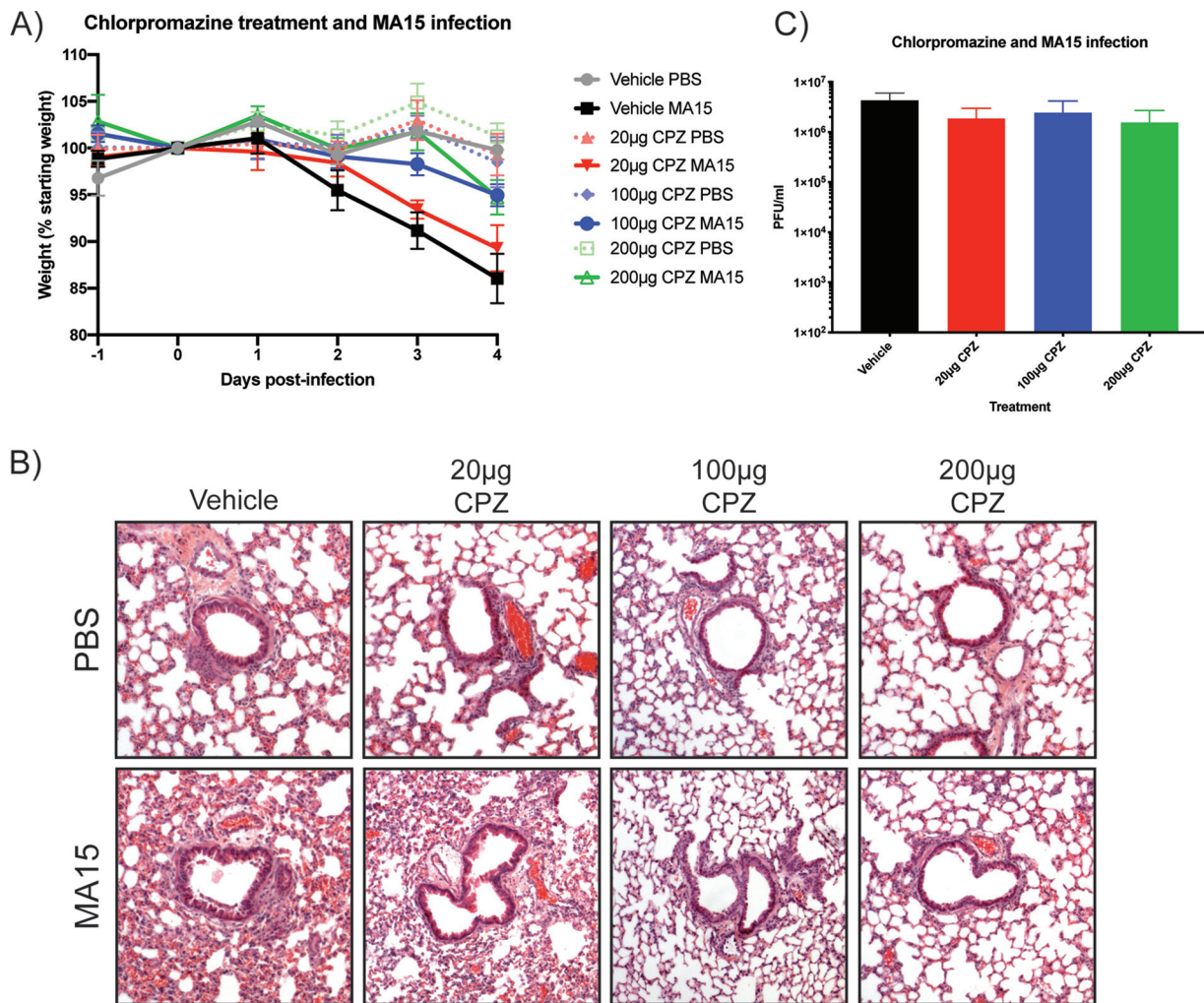


FIG 6 CQ is protective against SARS-CoV (MA15) disease *in vivo* but does not inhibit viral replication. As for Fig. 5, mice were treated with CPZ 1 day prior to infection with SARS-CoV (MA15) and through the 4-day infection time course. Water was used as the vehicle control for both drugs, and PBS was used as a control for uninfected mice. (A) Weight loss of mice treated with CPZ at three different doses (20 µg, 100 µg, and 200 µg) over the 4-day infection. Data are presented as relative weight loss compared to the mouse weight on day 0. In each treatment group, there were 5 mice, and data are means and standard deviations. (B) At day 4, mice were euthanized, and lung sections were used for H&E staining. (C) In addition to collecting lungs for section staining, there was also collection to determine titer of virus by plaque assay.

SARS-CoV MA15. There is currently a lack of a well-established mouse model for SARS-CoV-2, so we used the mouse-adapted SARS-CoV (MA15) strain as a surrogate to assess the *in vivo* efficacy of these drugs against a closely related coronavirus. We are of the opinion that this is a good model, since both viruses use ACE2 as a receptor (14–17) and therefore have similar cellular tropisms, which is important, since both of these compounds appear to inhibit viral entry. Prophylactic dosing in MA15 infection experiments demonstrated that, in contrast to the *in vitro* antiviral activity, CQ and CPZ did not inhibit viral replication in mouse lungs based on viral titers recovered at 4 dpi. However, both drugs resulted in reduced weight loss and improved clinical outcome, with the higher dose giving greater protection. Along with being an anti-malarial, CQ is used in humans for the treatment of systemic lupus erythematosus and rheumatoid arthritis because of its anti-inflammatory properties and effects on antigen presentation (19–21). We speculate that these properties may have a role in the protection we observed *in vivo*, since much of the pathology from SARS-CoV is a consequence of immunopathology during infection (in mice [22] and in nonhuman primates [23]; for a detailed review, see reference 24). Since CPZ treatment resulted in a similar phenotype, we speculate that its role as an inhibitor of clathrin-mediated endocytosis may have an

impact on cells of the immune system. HCQ and CQ have been examined in patients with COVID-19, and we are of the opinion that these drugs may not be viable therapeutics alone, since they do not inhibit viral replication in mouse lungs. However, the anti-inflammatory properties of these drugs, or other similar drugs, could potentially have a benefit for treatment of SARS-CoV-2 in combination with more directly acting antivirals, such as remdesivir (25–27). Chloroquine and hydroxychloroquine have become the source of much controversy for the treatment of COVID-19 and many studies suggest that they do not impact the course of disease (28–30). However, there are various ongoing clinical studies; a search on www.clinicaltrials.gov for “COVID-19 and hydroxychloroquine” returned close to 250 results. Our data suggest that in mice, chloroquine may have some impact on course of disease, but not on viral replication, when administered prophylactically. The need for prophylactic administration may mean that this is not a viable option in humans, but further clinical study is required.

The development of antiviral drugs for emerging coronaviruses is a global priority. In the midst of the COVID-19 pandemic, we must identify rapidly accessible therapeutics that are validated in both *in vitro* and *in vivo* models. FDA-approved drugs being assessed for repurposing and other experimental drugs in development must be properly validated in animal studies to best assess their potential utility in people. We present here a list of FDA-approved drugs that are effective *in vitro* against SARS-CoV-2 as well as being effective against SARS-CoV and MERS-CoV (6). Moreover, we have demonstrated that two of these, CQ and CPZ, can protect mice from severe clinical disease from SARS-CoV. Future research will be aimed at testing these compounds in SARS-CoV-2 animal models to further assess their potential utility for human treatment.

MATERIALS AND METHODS

Cell lines and virus. Vero E6 cells (ATCC CRL 1586) were cultured in Dulbecco's modified Eagle medium (DMEM; Quality Biological), supplemented with 10% (vol/vol) fetal bovine serum (Sigma), 1% (vol/vol) penicillin-streptomycin (Gemini Bio-products), and 1% (vol/vol) L-glutamine (2 mM final concentration; Gibco). A549-hACE2 cells were cultured in DMEM with 10% fetal bovine serum and 1% penicillin-streptomycin. Cells were maintained at 37°C and 5% CO₂. Samples of SARS-CoV-2 were obtained from the CDC following isolation from a patient in Washington State (WA-1 strain; BEI number NR-52281). Stocks were prepared by infection of Vero E6 cells for 2 days when cytopathic effect (CPE) was starting to be visible. Media were collected and clarified by centrifugation prior to being aliquoted for storage at –80°C. The titer of the stock was determined by plaque assay using Vero E6 cells as described previously (31). All work with infectious virus was performed in a biosafety level 3 laboratory and approved by our institutional biosafety committee. SARS-CoV stock was prepared as previously described (32). SARS-CoV spike (S) pseudotype viruses were produced as previously described (9).

Drug testing. All drug screens were performed with Vero E6 cells. Cells were plated in opaque 96-well plates 1 day prior to infection. Drug stocks were made in either dimethyl sulfoxide (DMSO), water, or methanol. Drugs were diluted from stock to 50 μM and an 8-point 1:2 dilution series made. Cells were pretreated with drug for 2 h at 37°C and 5% CO₂ prior to infection at an MOI of 0.01 or 0.004. Vehicle controls were used on every plate, and all treatments were performed in triplicate for each screen. In addition to plates that were infected, parallel plates were left uninfected to monitor cytotoxicity of drug alone. Three independent screens with this setup were performed. Cells were incubated at 37°C and 5% CO₂ for 3 days before CellTiter-Glo (CTG) assays were performed as per the manufacturer's instructions (Promega). Luminescence was read using a Molecular Devices SpectraMax L plate reader. Fluphenazine dihydrochloride, benzotropine mesylate, amodiaquine hydrochloride, amodiaquine dihydrochloride dihydrate, thiethylperazine maleate, mefloquine hydrochloride, triparanol, teronazole Vetrinal, anisomycin, flupirilene, clomipramine hydrochloride, hydroxychloroquine sulfate, promethazine hydrochloride, emetine dihydrochloride hydrate, and chloroquine phosphate were all purchased from Sigma. Chlorpromazine hydrochloride, toremifene citrate, tamoxifen citrate, gemcitabine hydrochloride, and imatinib mesylate were all purchased from Fisher Scientific.

Data analysis. Cytotoxicity data were normalized according to cell-only uninfected controls and CTG medium-only (blank) controls: $\{1 - [(drug - blank)/(cell\ only - blank)]\} \times 100$. Inhibition data were normalized according to cell-only data and the activity of the vehicle controls: $[(drug - vehicle)/(cell\ only - vehicle)] \times 100$.

Nonlinear regression analysis was performed on the normalized percent inhibition and cytotoxicity data, and IC₅₀s and half-maximal cytotoxic concentrations (CC₅₀s) were calculated from fitted curves (log[agonist] versus response – variable slope [four parameters]) (GraphPad Software, La Jolla, CA), as described previously (33). Drug dilution points in a given run were excluded from IC₅₀ analysis if the average cytotoxicity was greater than 30% (arbitrary cutoff) across the 3 cytotoxicity replicates for that screen. IC₅₀s or CC₅₀s extrapolated outside the drug dilution range tested were reported as greater than 50 μM or less than 0.39 μM. Selectivity indexes (SI) were also calculated by dividing the CC₅₀ by the IC₅₀.

Viral infection. To further analyze candidate drugs, Vero E6 or A549-hACE2 cells were grown in 24-well plate format for 24 h prior to infection. As with the drug screens, cells were pretreated with drug at various concentrations or with vehicle control for 2 h. Cells were then infected with SARS-CoV-2 at an MOI of 0.1 for 24 h for Vero E6 or 48 h for A549-hACE2 cells. Supernatant was collected, centrifuged in a tabletop centrifuge for 3 min at maximum speed and stored at -80°C . After a wash in PBS, infected cells were collected in TRIzol (Ambion) for RNA analysis (described below). Supernatant was used to determine the titers of viral production by TCID₅₀ assay (31).

RNA extraction and qRT-PCR. RNA was extracted from TRIzol samples using a Direct-zol RNA miniprep kit (Zymo Research) as per the manufacturer's instructions. RNA was converted to cDNA using a RevertAid RT kit (Thermo Scientific), with 12 μl of extracted RNA per reaction. For quantitative reverse transcription-PCR (qRT-PCR), 2 μl of cDNA reaction product was mixed with PowerUp SYBR green master mix (Applied Biosystems) and WHO/Corman primers targeting N and RdRp: N FWD, 5'-CACATTGGCAC CCGCAATC-3'; N REV, 5'-GAGGAACGAGAAGAGGCTTG-3'; RdRp FWD, 5'-GTGARATGGTCATGTGTGGCGG-3'; RdRp REV, 5'-CARATGTTAAASACACTATTAGCATA-3'. The qRT-PCRs were performed with a QuantStudio 5 system (Applied Biosystems). To normalize loading, 18S or GAPDH RNA were used as a control and was assessed with TaqMan gene expression assays (Applied Biosystems) and a TaqMan Fast Advanced master mix. Fold change between drug treated and vehicle control was determined by calculating $\Delta\Delta\text{C}_T$ after normalization to the endogenous control of 18S.

Pseudovirus fusion and entry assay. The pseudovirion (PV) entry assay was performed as described elsewhere (9, 34). Briefly, 2×10^4 BSC1 cells per well were in 96-well plates for 24 h, after which time cells were pretreated with drug (1 h) and infected with PV (3 h). Medium was removed, and cells were washed with loading buffer (47 ml clear DMEM, 5 mM probenecid, 2 mM L-glutamine, 25 mM HEPES, 200 nM bafilomycin, 5 μM E64D) and incubated for 1 h in CCF2 solution (LB, CCF2-AM, solution B [CCF2-AM kit K1032]; Thermo Fisher) in the dark. Cells were washed once with loading buffer and incubated from 6 h to overnight with 10% fetal bovine serum (FBS) in loading buffer. Percent CCF2 cleavage was assessed by flow cytometry on an LSRII flow cytometer (Beckton Dickinson) in the flow cytometry core facility at the University of Maryland, Baltimore. Data were analyzed using FlowJo.

Mouse infections. All infections were performed in an animal biosafety level 3 facility at the University of Maryland, Baltimore, using appropriate practices, including use of a HEPA-filtered bCON caging system, HEPA-filtered powered air-purifying respirators (PAPRs), and Tyvek suiting. All animals were grown to 10 weeks of age prior to use in experiments. The animals were anesthetized using a mixture of xylazine (0.38 mg/mouse) and ketamine (1.3 mg/mouse) in a 50- μl total volume by intraperitoneal injection. The mice were inoculated intranasally with 50 μl of either PBS or 2.5×10^3 PFU of rMA15 SARS-CoV (11), after which all animals were monitored daily for weight loss. Mice were euthanized 4 dpi, and lung tissue was harvested for further analysis. All animals were housed and used in accordance with the University of Maryland, Baltimore, Institutional Animal Care and Use Committee guidelines. Histological evaluation was performed in a blinded manner on duplicate lung sections for each of 5 mice per group at indicated time points. Representative images are presented.

Plaque assay. Vero cells were seeded in 35-mm dishes with 5×10^5 cells per dish 24 h prior to infection. Supernatants from homogenized were serially diluted 10^{-1} through 10^{-6} in serum-free (SF) medium. Cells were washed with SF medium, 200 μl of diluted virus was added to each well, and adsorption was allowed to proceed for 1 h at 37°C with gentle rocking every 10 min. DMEM (2 \times) and 1.6% agarose were mixed 1:1. Cells were washed with SF medium, 2 ml DMEM-agarose was added to each well, and cells were incubated for 72 h at 37°C , after which time plaques were read.

Statistical analysis. All statistical analysis was performed with GraphPad software (GraphPad, La Jolla, CA).

ACKNOWLEDGMENTS

We kindly thank Emergent BioSolutions for financial support to perform these experiments. S.W. is supported by R01-AI-140442. M.B.F. is supported by BMGF INV-006099, ASPR-20-01495, NIAID contract 75N93019C00051, and DARPA HR0011-20-2-0040.

We also kindly thank Julie Dyall for helpful discussions regarding data analysis.

Investigation, S.W., C.C., R.H., J.L., K.M.; Conceptualization & methodology, S.W., C.C., M.F.; Writing – original draft, S.W., M.F.; Writing – Review & Editing, S.W., C.C., R.H., J.L., M.F.

We declare no competing interests.

REFERENCES

- Zhu N, Zhang D, Wang W, Li X, Yang B, Song J, Zhao X, Huang B, Shi W, Lu R, Niu P, Zhan F, Ma X, Wang D, Xu W, Wu G, Gao GF, Tan W, China Novel Coronavirus Investigating and Research Team. 2020. A novel coronavirus from patients with pneumonia in China, 2019. *N Engl J Med* 382:727–733. <https://doi.org/10.1056/NEJMoa2001017>.
- Sisk JM, Frieman MB. 2016. Screening of FDA-approved drugs for treatment of emerging pathogens. *ACS Infect Dis* 1:401–402. <https://doi.org/10.1021/acsinfecdis.5b00089>.
- Pushpakom S, Iorio F, Eyers PA, Escott KJ, Hopper S, Wells A, Doig A, Guilliams T, Latimer J, McNamee C, Norris A, Sanseau P, Cavalla D, Pirmohamed M. 2019. Drug repurposing: progress, challenges and recommendations. *Nat Rev Drug Discov* 18:41–58. <https://doi.org/10.1038/nrd.2018.168>.
- Mercorelli B, Palù G, Loregian A. 2018. Drug repurposing for viral infectious diseases: how far are we? *Trends Microbiol* 26:865–876. <https://doi.org/10.1016/j.tim.2018.04.004>.

5. Madrid PB, Chopra S, Manger ID, Gilfillan L, Keepers TR, Shurtleff AC, Green CE, Iyer LV, Dilks HH, Davey RA, Kolokoltsov AA, Carrion R, Patterson JL, Bavari S, Panchal RG, Warren TK, Wells JB, Moos WH, Burke RLL, Tanga MJ. 2013. A systematic screen of FDA-approved drugs for inhibitors of biological threat agents. *PLoS One* 8:e60579. <https://doi.org/10.1371/journal.pone.0060579>.
6. Dyall J, Coleman CM, Hart BJ, Venkataraman T, Holbrook MR, Kindrachuk J, Johnson RF, Olinger GG, Jahrling PB, Laidlaw M, Johansen LM, Lear-Rooney CM, Glass PJ, Hensley LE, Frieman B. 2014. Repurposing of clinically developed drugs for treatment of Middle East respiratory syndrome coronavirus infection. *Antimicrob Agents Chemother* 58:4885–4893. <https://doi.org/10.1128/AAC.03036-14>.
7. Madrid PB, Panchal RG, Warren TK, Shurtleff AC, Endsley AN, Green CE, Kolokoltsov A, Davey R, Manger ID, Gilfillan L, Bavari S, Tanga MJ. 2015. Evaluation of Ebola virus inhibitors for drug repurposing. *ACS Infect Dis* 1:317–326. <https://doi.org/10.1021/acinfeddis.5b00030>.
8. Xu M, Lee EM, Wen Z, Cheng Y, Huang WK, Qian X, Tcw J, Kouznetsova J, Ogden SC, Hammack C, Jacob F, Nguyen HN, Itkin M, Hanna C, Shinn P, Allen C, Michael SG, Simeonov A, Huang W, Christian KM, Goate A, Brennand KJ, Huang R, Xia M, Ming GL, Zheng W, Song H, Tang H. 2016. Identification of small-molecule inhibitors of Zika virus infection and induced neural cell death via a drug repurposing screen. *Nat Med* 22:1101–1107. <https://doi.org/10.1038/nm.4184>.
9. Coleman CM, Sisk JM, Mingo RM, Nelson EA, White JM, Frieman MB. 2016. Abl kinase inhibitors are potent inhibitors of SARS-CoV and MERS-CoV fusion. *J Virol* 90:8924–8933. <https://doi.org/10.1128/JVI.01429-16>.
10. Sisk JM, Frieman MB, Machamer CE. 2018. Coronavirus S protein-induced fusion is blocked prior to hemifusion by Abl kinase inhibitors. *J Gen Virol* 99:619–630. <https://doi.org/10.1099/jgv.0.001047>.
11. Roberts A, Deming D, Paddock CD, Cheng A, Yount B, Vogel L, Herman BD, Sheahan T, Heise M, Genrich GL, Zaki SR, Baric R, Subbarao K. 2007. A mouse-adapted SARS-coronavirus causes disease and mortality in BALB/c mice. *PLoS Pathog* 3:e5. <https://doi.org/10.1371/journal.ppat.0030005>.
12. Pastick KA, Okafor EC, Wang F, Lofgren SM, Skipper CP, Nicol MR, Pullen MF, Rajasingham R, McDonald EG, Lee TC, Schwartz IS, Kelly LE, Lother SA, Mitjà O, Letang E, Abassi M, Boulware DR. 2020. Review: hydroxychloroquine and chloroquine for treatment of SARS-CoV-2 (COVID-19). *Open Forum Infect Dis* 7:ofaa130. <https://doi.org/10.1093/ofid/ofaa130>.
13. Wang LH, Rothberg KG, Anderson RGW. 1993. Mis-assembly of clathrin lattices on endosomes reveals a regulatory switch for coated pit formation. *J Cell Biol* 123:1107–1117. <https://doi.org/10.1083/jcb.123.5.1107>.
14. Li W, Moore MJ, Vasilieva N, Sui J, Wong SK, Berne MA, Somasundaran M, Sullivan JL, Luzuriaga K, Greenough TC, Choe H, Farzan M. 2003. Angiotensin-converting enzyme 2 is a functional receptor for the SARS coronavirus. *Nature* 426:450–454. <https://doi.org/10.1038/nature02145>.
15. Zhou P, Yang X-L, Wang X-G, Hu B, Zhang L, Zhang W, Si H-R, Zhu Y, Li B, Huang C-L, Chen H-D, Chen J, Luo Y, Guo H, Jiang R-D, Liu M-Q, Chen Y, Shen X-R, Wang X, Zheng X-S, Zhao K, Chen Q-J, Deng F, Liu L-L, Yan B, Zhan F-X, Wang Y-Y, Xiao G-F, Shi Z-L. 2020. A pneumonia outbreak associated with a new coronavirus of probable bat origin. *Nature* 579:270–273. <https://doi.org/10.1038/s41586-020-2012-7>.
16. Wan Y, Shang J, Graham R, Baric RS, Li F. 2020. Receptor recognition by the novel coronavirus from Wuhan: an analysis based on decade-long structural studies of SARS coronavirus. *J Virol* 94:e00127-20. <https://doi.org/10.1128/JVI.00127-20>.
17. Hoffmann M, Kleine-Weber H, Schroeder S, Krüger N, Herrler T, Erichsen S, Schiergens TS, Herrler G, Wu NH, Nitsche A, Müller MA, Drosten C, Pöhlmann S. 2020. SARS-CoV-2 cell entry depends on ACE2 and TMPRSS2 and is blocked by a clinically proven protease inhibitor. *Cell* 181:271–280 E8. <https://doi.org/10.1016/j.cell.2020.02.052>.
18. Baird JK. 2005. Effectiveness of antimalarial drugs. *N Engl J Med* 352:1565–1577. <https://doi.org/10.1056/NEJMra043207>.
19. Ziegler HK, Unanue ER. 1982. Decrease in macrophage antigen catabolism caused by ammonia and chloroquine is associated with inhibition of antigen presentation to T cells. *Proc Natl Acad Sci U S A* 79:175–178. <https://doi.org/10.1073/pnas.79.1.175>.
20. Al-Bari MAA. 2015. Chloroquine analogues in drug discovery: new directions of uses, mechanisms of actions and toxic manifestations from malaria to multifarious diseases. *J Antimicrob Chemother* 70:1608–1621. <https://doi.org/10.1093/jac/dkv018>.
21. Rainsford KD, Parke AL, Clifford-Rashotte M, Kean WF. 2015. Therapy and pharmacological properties of hydroxychloroquine and chloroquine in treatment of systemic lupus erythematosus, rheumatoid arthritis and related diseases. *Inflammopharmacology* 23:231–269. <https://doi.org/10.1007/s10787-015-0239-y>.
22. Rockx B, Baas T, Zornetzer GA, Haagmans B, Sheahan T, Frieman M, Dyer MD, Teal TH, Proll S, van den Brand J, Baric R, Katze MG. 2009. Early upregulation of acute respiratory distress syndrome-associated cytokines promotes lethal disease in an aged-mouse model of severe acute respiratory syndrome coronavirus infection. *J Virol* 83:7062–7074. <https://doi.org/10.1128/JVI.00127-09>.
23. Smits SL, De Lang A, Van Den Brand JMA, Leijten LM, Van Ijcken WF, Eijkemans MJC, Van Amerongen G, Kuiken T, Andeweg AC, Osterhaus ADME, Haagmans BL. 2010. Exacerbated innate host response to SARS-CoV in aged non-human primates. *PLoS Pathog* 6:e1000756. <https://doi.org/10.1371/journal.ppat.1000756>.
24. Channappanavar R, Perlman S. 2017. Pathogenic human coronavirus infections: causes and consequences of cytokine storm and immunopathology. *Semin Immunopathol* 39:529–539. <https://doi.org/10.1007/s00281-017-0629-x>.
25. Wang M, Cao R, Zhang L, Yang X, Liu J, Xu M, Shi Z, Hu Z, Zhong W, Xiao G. 2020. Remdesivir and chloroquine effectively inhibit the recently emerged novel coronavirus (2019-nCoV) in vitro. *Cell Res* 30:269–271. <https://doi.org/10.1038/s41422-020-0282-0>.
26. Brown AJ, Won JJ, Graham RL, Dinnon KH, Sims AC, Feng JY, Cihlar T, Denison MR, Baric RS, Sheahan TP. 2019. Broad spectrum antiviral remdesivir inhibits human endemic and zoonotic deltacoronaviruses with a highly divergent RNA dependent RNA polymerase. *Antiviral Res* 169:104541. <https://doi.org/10.1016/j.antiviral.2019.104541>.
27. Sheahan TP, Sims AC, Graham RL, Menachery VD, Gralinski LE, Case JB, Leist SR, Pyrc K, Feng JY, Trantcheva I, Bannister R, Park Y, Babusis D, Mo C, MacKman RL, Spahn JE, Palmiotti CA, Siegel D, Ray AS, Cihlar T, Jordan R, Denison MR, Baric RS. 2017. Broad-spectrum antiviral GS-5734 inhibits both epidemic and zoonotic coronaviruses. *Sci Transl Med* 9:eal3653. <https://doi.org/10.1126/scitranslmed.aal3653>.
28. Boulware DR, Pullen MF, Bangdiwala AS, Pastick KA, Lofgren SM, Okafor EC, Skipper CP, Nascene AA, Nicol MR, Abassi M, Engen NW, Cheng MP, LaBar D, Lother SA, MacKenzie LJ, Drobot G, Marten N, Zarychanski R, Kelly LE, Schwartz IS, McDonald EG, Rajasingham R, Lee TC, Hullsiek KH. 2020. A randomized trial of hydroxychloroquine as postexposure prophylaxis for Covid-19. *N Engl J Med* 383:517–525. <https://doi.org/10.1056/NEJMoa2016638>.
29. Cavalcanti AB, Zampieri FG, Rosa RG, Azevedo LCP, Veiga VC, Avezum A, Damiani LP, Marcadenti A, Kawano-Dourado L, Lisboa T, Junqueira DLM, de Barros e Silva PGM, Tramuja L, Abreu-Silva EO, Laranjeira LN, Soares AT, Echenique LS, Pereira AJ, Freitas FGR, Gebara OCE, Dantas VCS, Furat RHM, Milan EP, Golin NA, Cardoso FF, Maia IS, Hoffmann Filho CR, Kormann APM, Amazonas RB, Bocchi de Oliveira MF, Serpa-Neto A, Falavigna M, Lopes RD, Machado FR, Berwanger O. 2020. Hydroxychloroquine with or without azithromycin in mild-to-moderate Covid-19. *N Engl J Med* 2020:NEJMoa2019014. Epub ahead of print. <https://doi.org/10.1056/NEJMoa2019014>.
30. Geleris J, Sun Y, Platt J, Zucker J, Baldwin M, Hripcsak G, Labella A, Manson DK, Kubin C, Barr RG, Sobieszczyk ME, Schluger NW. 2020. Observational study of hydroxychloroquine in hospitalized patients with COVID-19. *N Engl J Med* 382:2411–2418. <https://doi.org/10.1056/NEJMoa2012410>.
31. Coleman CM, Frieman MB. 2015. Growth and quantification of MERS-CoV infection. *Curr Protoc Microbiol* 37:15E.2.1–15E.2.9. <https://doi.org/10.1002/9780471729259.mc15e02s37>.
32. Frieman M, Yount B, Agnihotram S, Page C, Donaldson E, Roberts A, Vogel L, Woodruff B, Scorpio D, Subbarao K, Baric RS. 2012. Molecular determinants of severe acute respiratory syndrome coronavirus pathogenesis and virulence in young and aged mouse models of human disease. *J Virol* 86:884–897. <https://doi.org/10.1128/JVI.05957-11>.
33. Dyall J, Johnson JC, Hart BJ, Postnikova E, Cong Y, Zhou H, Gerhardt DM, Michelotti J, Honko AN, Kern S, DeWald LE, O'Loughlin KG, Green CE, Mirsalis JC, Bennett RS, Olinger GG, Jahrling PB, Hensley LE. 2018. In vitro and in vivo activity of amiodarone against Ebola virus. *J Infect Dis* 218:S592–S596. <https://doi.org/10.1093/infdis/jiy345>.
34. Mingo RM, Simmons JA, Shoemaker CJ, Nelson EA, Schornberg KL, D'Souza RS, Casanova JE, White JM. 2015. Ebola virus and severe acute respiratory syndrome coronavirus display late cell entry kinetics: evidence that transport to NPC1+ endolysosomes is a rate-defining step. *J Virol* 89:2931–2943. <https://doi.org/10.1128/JVI.03398-14>.